Polymer−Solvent Interactions in Phosphazene Materials As Observed by Solid- and Liquid-State NMR Spectroscopy

F. F Stewart,*,† E. S. Peterson,† S. C. Busse,‡ and C. J. Orme†

Idaho National Engineering Laboratory, Lockheed Martin Idaho Technologies Company, P.O. Box 1625, Idaho Falls, Idaho 83415-2208, and Montana State University, Department of Chemistry and Biochemistry, Bozeman, Montana 59717

Received May 7, 1996. Revised Manuscript Received August 21, 1996[⊗]

The chemical nature of the interactions between materials and occluded small molecules have been the subject of intense study. In this paper, we demonstrate the utility of NMR spectroscopy for examining dynamic systems. Phosphazenes are inorganic polymers with an alternating nitrogen−phosphorus backbone that may be tailored by substitution of differing organic pendant groups, thus assuming a variety of physical and chemical characteristics. We examine two examples of phosphazenes and determine that solvents that penetrate and swell will influence the material at the molecular level. It has been determined that solvation in swollen materials is complete and can be observed by NMR spectroscopy. Variable-temperature NMR spectroscopy and nuclear relaxation phenomena demonstrate motional dynamics within the polymer matrix. In addition, reorientation rates are enhanced and the free volume within the matrix is increased with the inclusion of solvent. Additional evidence for solvation is observed through the use of heterogeneous-phase NOE difference spectroscopy where a dipolar interaction between solvent and substrate yields internuclear distances of less than 5 Å. These data lend support to the solution-diffusion model as a mechanism for permeation and transport of small molecules within a polymer matrix.

Introduction

Polymer−solvent interactions have been and remain the subject of considerable interest in the scientific community. Reasons for such interest include polymer processing, barriers, and semipermeable membranes. The majority of authors have concerned themselves with determining thermodynamic and interaction parameters.[1−3] Several authors have dealt with molecular "sticking" parameters. A subset of these studies has used NMR spectroscopy.[4] However, few studies deal with both polymer interactions and evaluation of polymeric materials for membrane applications using NMR spectroscopy. The set of studies outlined in this paper provides the basis for evaluating polymers for membrane applications. NMR spectroscopy was chosen as a tool for these studies due to its unique ability to provide direct observation of molecular interactions in dynamic systems.

Solution-diffusion theory[5] suggests that permeation of an analyte through a polymer matrix can be thought of as a three-step process: adsorption of the analyte onto the polymer, diffusion through the polymer matrix, and desorption from the polymer. The ability to observe directly this behavior has been limited; therefore, the ability to predict polymer membrane performance has been a problem. In this paper, we report that the physical characteristics of phosphazene polymers exhibit dramatic changes upon swelling in solvent. These differences are reflected by variable-temperature solid-state CPMAS nuclear magnetic resonance (NMR) spectra and through ^{13}C and ^{1}H $T_{1\rho}$ relaxation measurements. The points of solvent−polymer interaction are delineated using nuclear Overhauser effect (NOE) experiments.

The inorganic membrane technology research program (IMTRP) at the Idaho National Engineering Laboratory (INEL) is dedicated to understanding transport properties of polymer membranes for energy conservation and environmental applications. Polyphosphazenes offer an ideal platform for the construction of "custom-tailored" polymers. Their phosphorus−nitrogen backbone is chemically and thermally stable compared to organic polymers. In addition, they are easy to substitute with organic and inorganic substituents, thus providing a variety of physical properties.[6] The IMTRP has studied phosphazene membranes in both flat-sheet and tubular formats for chemical-separations applications for the past several years. Nearly all of the studies have been upon dense films of the materials. The applications studied have included gas separations, liquid−liquid separations, and solid−liquid separations. For the area of gas separations, it was found that both the rubbery linear and glassy cyclomatrix phosphazenes

[⊗] Abstract published in *Advance ACS Abstracts,* October 1, 1996.

(1) McCall, D. W. *Mol. Relaxation Polym.* **1971**, *4*, 223.
(2) Fyfe, C. A.; Lyerla, J. R.; Volksen, W.; Yannoni, C. S *Aromatic Polyesters* **1979**, *12*, 4.
(3) Claves, J.; Schmidt-Rohr, K.; Adam, A.; Boeffel, C; Spiess, H. W. *Macromolecules* **1992**, *25*, 5208.
(4) (a) Young, S. C.; Magill, J. H. *Macromolecules* **1989**, *22*, 2549. (b) Ganapathy, S.; Ray, S. S.; Rajamohanan, P. R.; Mashelker, R. A. *J. Phys. Chem* **1995**, *103* (15), 6783.
(5) Park, G. S. In *Synthetic Membranes: Science, Engineering, and Applications*; Bungay, P. M., Lonsdale, H. K., DePinho, M. N., Eds.; NATO A.S.I. Series; D. Reidel Publishing Co.: Dordrecht, 1983; pp 57−108.
(6) Mark, J. E.; Allcock, H. R.; West, R. *Inorganic Polymers*; Prentice Hall: Englewood Cliffs, NJ, 1992.

S0897-4756(96)00266-9 CCC: $14.00

offered a reasonable set of materials for high temperature (up to 250 °C) separations with good fluxes and selectivities for both acid gases and longer chain hydrocarbons.[7−14] Assuming solution-diffusion theory is valid, the separation mechanism is based upon a dominance of the sorption factor over the diffusive. In the area of liquid separations, several areas continue to be explored including reverse osmosis, nanofiltration, and pervaporation. Specific areas of focus have included halogenated hydrocarbon−water separations for which separation factors of 10 000 or greater have been observed.[15−17] Mechanistic studies have shown a solution-diffusion explanation as being most appropriate. Also included in the list are alcohol−dye separations for which dye rejections of greater than 99.9% are regularly observed.[18,19] The means of separation for this work is best described as a combination of convective and diffusive mechanisms.[18] Nonetheless, determination of polymer suitability for a specific separation application remains a very time-consuming step. This paper proposes that solid- and liquid-state NMR techniques can be combined to provide a novel, rapid, initial polymer screening method that is generally applicable to polymers for membrane applications. To address this question, three well-characterized solvent systems, referenced above, were chosen for study including halogenated hydrocarbons, 2-propanol, and tetrahydrofuran.

Diffusivity and solubility of a permeant, two factors that affect the rate of permeation,[20] are influenced by both the chemical composition of the polymer and the free volume within the matrix. Polymer swelling, or the inclusion of solvent within the polymer matrix, increases the free volume of the polymer available for transport which can lower the activation energy for permeation.[21−23] Probable mechanisms for molecular diffusion have been described in terms of several models that generally fall into two categories.

Table 1. Assignment of Carbon-13 NMR Data for the PPOP and PPXP Polymers

carbon	PPOP phenoxy group (ppm)	PPXP *p-sec*-butylphenoxy group (ppm)	*p*-methoxyphenoxy group (ppm)
ortho	120	122	114
meta	126	128	123
para	118	143	146
ipso (oxygen bearing)	148	151	156
methoxy methyl			51
α-methine		38	
β-methylene		28	
β-methyl		19	
γ-methyl		9	

The molecular model describes transport by a vibrational mechanism.[24−26] In this model, transport is described according to the size of the molecule being transported, and the vibrational motions of the polymer chains and side groups. Diffusion is portrayed as an activated process by this model, because it is dependent upon temperature. Conversely, the free-volume model describes transport as occurring due to random fluctuation of free volume within the polymer matrix.[27] The free volume within the polymeric matrix can be thought of as intermolecular defects in the polymer structure ranging from branch points, cross-links, and chemical imperfections in the polymer chain (side groups and end groups) to discrete pores. These defects act as cages that the penetrant molecule can occupy. Transport occurs from one cage to another due to random vibrations and density fluctuations of the matrix.

Nuclear relaxation mechanisms give insight into molecular processes and motions. Numerous solid-state NMR spectroscopic methods have been employed to describe molecular motions within polymers with varying degrees of success.[1,28−36] Rothwell and Waugh[37] have determined correlation times based upon observed line widths over a broad range of temperatures. Relaxation times of carbons and protons in the rotating frame, $T_{1\rho}$, have been shown to correlate to molecular motion.[28,29,33,34,36] Both parameters are valuable indicators of molecular motion with one clear distinction. ^{1}H $T_{1\rho}$ suffers from efficient spin-diffusion processes which average signals for different sites. Thus, localization

(7) Allen, C. A.; McCaffrey, R. R.; Cummings, D. G.; Grey, A. E.; Jessup, J. S.; McAtee, R. E. US Patent 4,749,489, 1988.
(8) McCaffrey, R. R.; Cummings, D. G. *Sep. Sci. Technol.* **1988**, *23*, 1627.
(9) Allen, C. A.; Cummings, D. G.; Grey, A. E.; McAtee, R. E.; McCaffrey, R. R. *J. Membr. Sci.* **1987**, *33*, 181.
(10) McCaffrey, R. R.; McAtee, R. E.; Grey, A. E.; Allen, C. A.; Cummings, D. G.; Applehans, A. D. *J. Membr. Sci.* **1986**, *28*, 47.
(11) McCaffrey, R. R.; McAtee, R. E.; Grey, A. E.; Allen, C. A.; Cummings, D. G.; Applehans, A. D.; Wright, R. B.; Jolley, J. G. *Sep. Sci. Technol.* **1987**, *22*, 873.
(12) Peterson, E. S.; Stone, M. L. *J. Membr. Sci.* **1994**, *86*, 57.
(13) Peterson, E. S.; Stone, M. L.; McCaffrey, R. R.; Cummings, D. G. *Sep. Sci. Technol.* **1993**, *28*, 1−3.
(14) Peterson, E. S.; Stone, M. L.; Orme, C. J.; Reavill, D. A., III, *Sep. Sci. Technol.* **1995**, *30* (7−9), 1573.
(15) Peterson, E. S.; Stone, M. L.; Bauer, W. F.; Orme, C. J. *Rec. Prog. Geni ds Proc., Membr. Processes* **1992**, *6* (22), 381.
(16) Peterson, E. S.; Stone, M. L.; McCaffrey, R. R.; Cummings, D. G. *Sep. Sci. Technol.* **1993**, *28*, 1−3.
(17) McCaffrey, R. R.; Cummings, D. G. US Patent 5,022,996, 1991 (pervap).
(18) Peterson, E. S.; Stone, M. L.; Orme, C. J.; Stewart, F. F.; Cowan, R. L. *Sep. Sci. Technol.*, in press.
(19) Peterson, E. S.; Stone, M. L.; Orme, C. J. U.S. Patent 5,385,672, 1995.
(20) Mulder, M. H. V. In *Pervaporation Membrane Separation Processes*; Huang, R. Y. M., Ed.; Elsevier: Amsterdam, 1991; pp 225−250.
(21) Brown, W. *Biochem. J.* **1915,** *9*, 591.
(22) Eustache, H.; Histi, G. *J. Membr. Sci.* **1981**, *8*, 105.
(23) Huang, R. Y. M.; Rhim, J. W. In *Pervaporation Membrane Separation Processes*; Huang, R. Y. M., Ed.; Elsevier: Amsterdam, 1991; p 111.
(24) Barrer, R. M. *J. Phys. Chem.* **1957,** *61*, 178.
(25) Brandt, W. W. *J. Phys. Chem.* **1959**, *63*, 1080.
(26) DiBenedetto, A. T. *J. Polym. Sci.: Part A* **1963,** *1*, 3459.
(27) Fugita, H. In *Diffusion in Polymers*; Crank, J.; Park, S., Eds.; Academic Press: New York, 1968; p 75.
(28) Stejkal, E. O.; Schaefer, J.; Sefcik, M. D.; McKay, R. A. *Macromolecules* **1981**, *14*, 275.
(29) Schaefer, J.; Stejkal, E. O.; Buchdahl, R. *Macromolecules* **1977**, *10*, 384.
(30) Fleming, W. W.; Lyerla, J. R.; Yannoni, C. S. In *NMR and Macromolecules: Sequence, Dynamic, and Domain Structure*; Randall, J. C., Ed.; American Chemical Society: Washington DC, 1984; p 83.
(31) Gambogi, J. E.; Blum, F. D. *Macromolecules* **1992**, *25*, 4526.
(32) Tarpley, M. F.; Lin, Y.-Y.; Jones, A. A.; Inglefield, In *NMR and Macromolecules: Sequence, Dynamic, and Domain Structure*; Randall, J. C., Ed.; American Chemical Society: Washington DC, 1984; p 67.
(33) Sefcik, M. D.; Schaefer, J.; Stejkal, E. O.; McKay, R. A. *Macromolecules* **1980**, *13*, 1132.
(34) Schaefer, J.; Sefcik, M. D.; Stejkal, E. O.; McKay, R. A. *Macromolecules* **1981**, *14*, 188.
(35) Earl, W. L.; Van der Hart, D. L. *Macromolecules* **1979**, *12*, 384.
(36) Steger, T.; Schaefer, J.; Stejkal, E. O.; McKay, R. A. *Macromolecules* **1980**, *13*, 1127.
(37) Rothwell, W. P.; Waugh, J. S. *J. Chem. Phys.* **1981**, *74*, 2721.

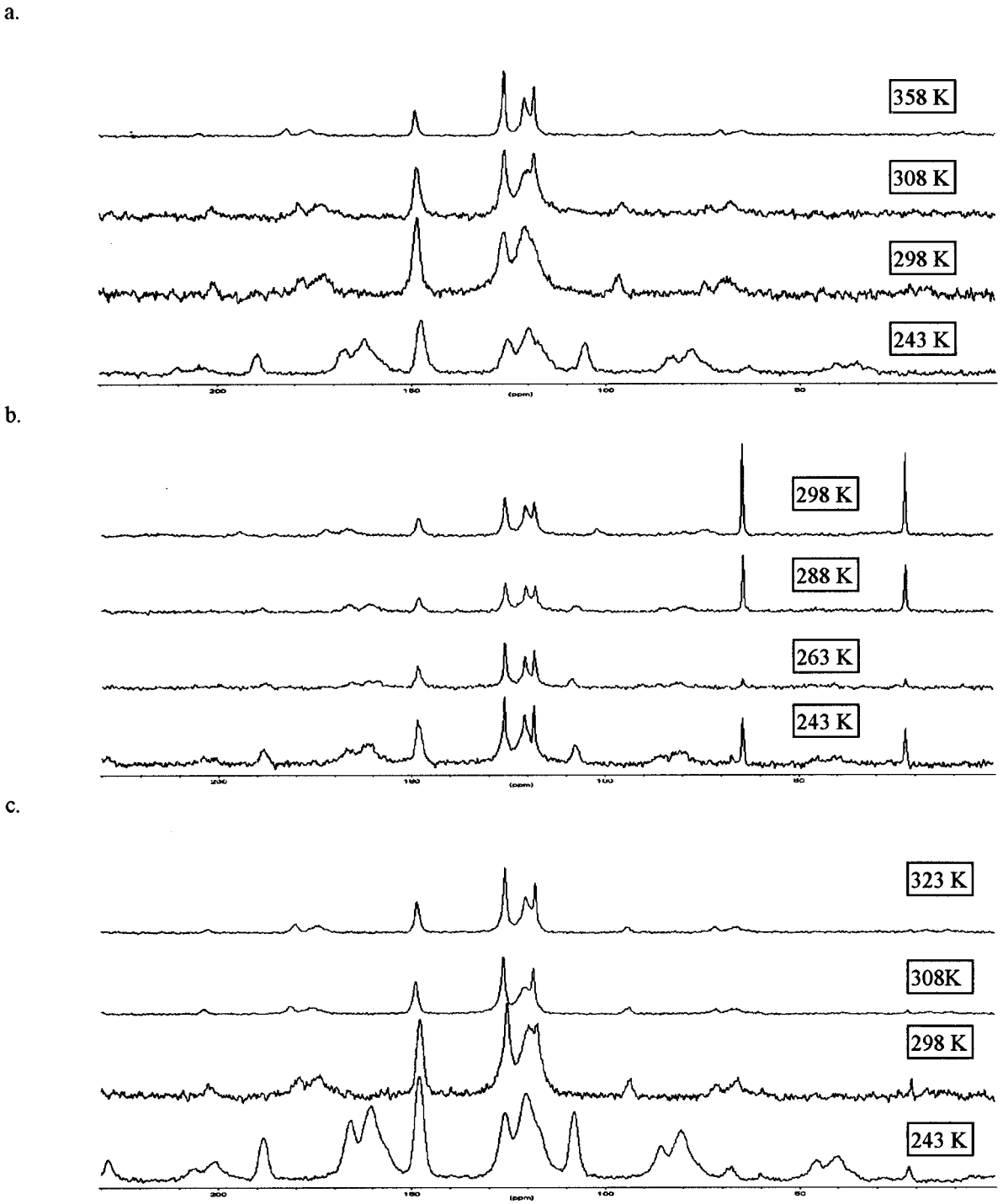

Figure 1. Variable-temperature ^{13}C CPMAS NMR spectra of PPOP. (a) Dry PPOP. PPOP resonances are assigned between 150 and 110 ppm with spinning sideband manifold evident. (b) Exposed to THF. Signals at 23 and 65 ppm are assigned to THF. Signals assigned to PPOP are found at 148, 126, 120, and 118 ppm. Spinning sideband manifolds are observed both upfield and downfield of the PPOP signals. (c) 2-Propanol exposed. PPOP signal are assigned between 150 and 110 ppm with spinning sideband manifolds evident for all experiments. The sidebands have greater intensity at 243 K due to slower spinning rate (2.8 kHz) as compared to the higher temperature experiments (4.5 kHz).

of an individual interaction is not possible.[38] Stejkal and Schaefer[28] reported that ^{13}C $T_{1\rho}$ relaxation parameters are influenced by both spin−spin and spin−lattice relaxation pathways. This can be problematic because direct information concerning molecular motion can be derived only from spin−lattice relaxation measurements. Qualitatively, however, information from polymer swelling may be gathered from either relaxation mechanism.

NMR is unique in its ability to study dynamic systems in which there is chemical exchange. When a spin A is irradiated and exchanges magnetization with spin B, the steady-state magnetization at site B is given by[39]

(38) Strothers, J. B. *Carbon-13 NMR Spectroscopy*; Academic Press: New York, 1972; p 197.

(39) Sander, J. K. M.; Hunter, B. K. *Modern NMR Spectroscopy, A Guide for Chemists*; Oxford University Press: Oxford, 1987.

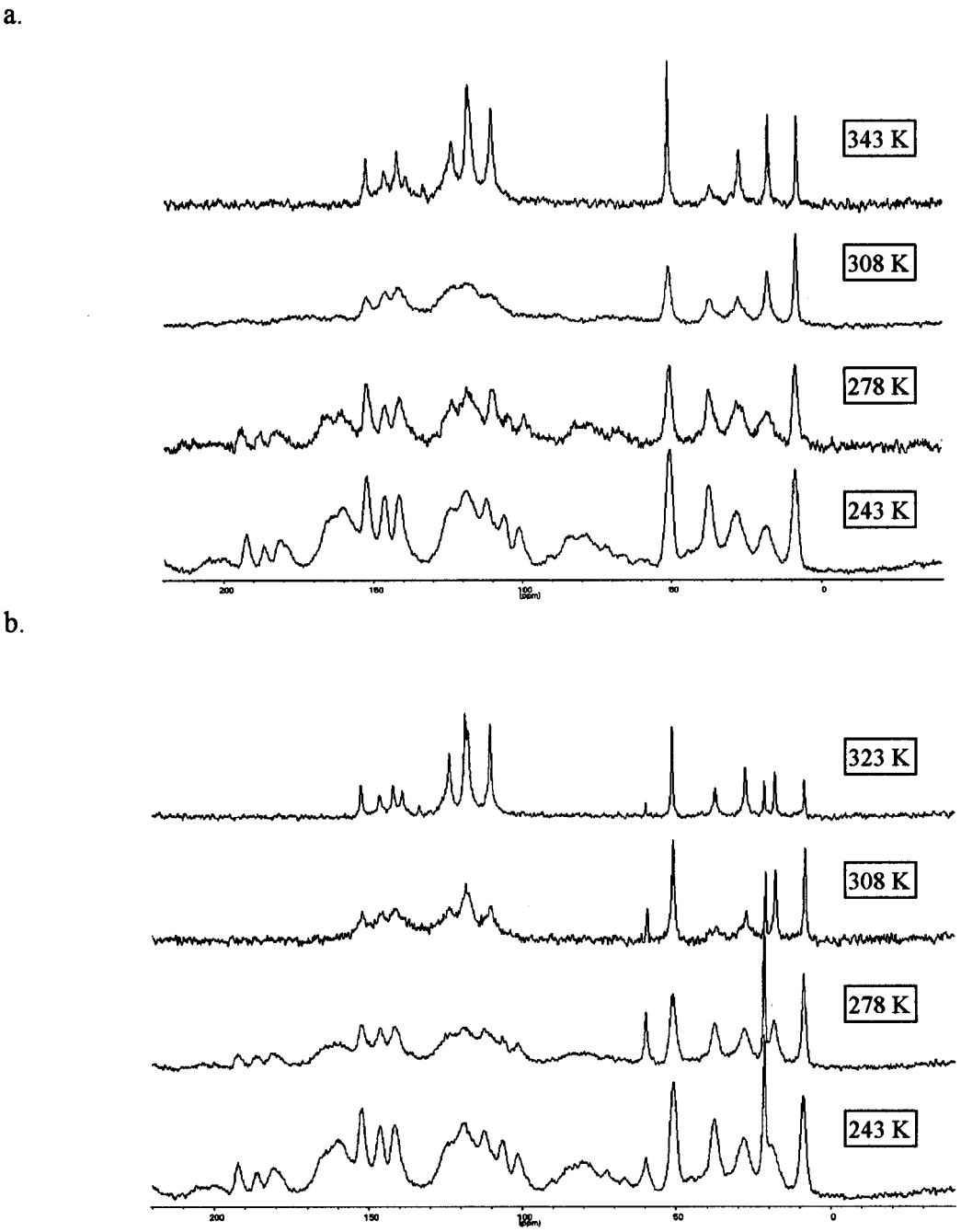

Figure 2. Variable-temperature ^{13}C CPMAS NMR spectra of PPXP. (a) Dry PPXP. Spinning sideband manifolds are prominent at 243 and 278 K due to slower spinning (2.8 versus 4.5 kHz for the higher temperature experiments. (b) 2-Propanol exposed PPXP. Spinning sidebands about the aromatic region are noticable with the slower spinning rate used for the two lower temperature experiments. Peaks at approximately 60 and 21 ppm are assigned to 2-propanol.

$$Mz_B/M_0 = R_{1B}/(R_{1B} + K_{AB}) \qquad (1)$$

where R_{1B} is the T_1 relaxation rate for spin B and K_{AB} is the effective first-order rate constant for the transfer from spin A to spin B. This transfer generally results in an enhancement due to increased magnetization. This enhancement is referred to the nuclear Overhauser effect (NOE). Individual exchanges may be queried using a one-dimensional difference technique. Typically, this technique has been applied to soluble species to give internuclear distances between atoms that are not *J*-coupled. In this paper, we present our findings on the application of NOE difference spectroscopy to a heterogeneous system.

Experimental Section

The polymers used for this study were (1) poly(bisphenoxy phosphazene) ORGAFLEX ADP 300 (PPOP), molecular weight (number average) 202 000, $T_g = -0.9$ °C. A thermal T_1 transition was observed at 125.0 °C, suggesting a degree of crystallinity within the polymer; and (2) cross-linkable polyphosphazene ORGAFLEX AMF 100 (PPXP), molecular weight (number average) 1 200 000, $T_g = -3.1$ °C; supplied by ELF ATOCHEM, S.A. PPXP is a terpolymer with the following approximate pendant group composition: 55% *p*-methoxyphenol, 36% *p-sec*-butylphenol, and 9% o-allylphenol. The addition of the *o*-allylphenol allows for cross-linking. These polymers were used as supplied without further purification. Both before and after cross-linking, PPXP is an amorphous dense film as a membrane that when cast, is generally 30 μm in thickness. All PPXP experiments were performed on cross-linked polymer. 2-Propanol, tetrahydrofuran, and methylene

Table 2. ^{13}C $T_{1\rho}$ Data for Dry and Solvent-Swelled PPOP Polymers

	dry PPOP (ms)			THF-swelled PPOP (ms)			2-propanol-swelled PPOP (ms)		
temp (K)	ipso 148 ppm	meta 126 ppm	ortho 118 ppm	ipso 148 ppm	meta 126 ppm	ortho 118 ppm	ipso 148 ppm	meta 126 ppm	ortho 118 ppm
343	71.5 ± 10	28.5 ± 2	28.4 ± 2						
323	32.9 ± 3	16.1 ± 1	16.9 ± 1				49.8 ± 2	22.5 ± 1	22.8 ± 2
308	29.1 ± 2	8.0 ± 1	8.6 ± 1				35.3 ± 2	12.4 ± 0.2	12.6 ± 0.3
298	13.0 ± 2	7.1 ± 1	8.3 ± 1	33.0 ± 1	28.7 ± 3	19.3 ± 2	44.5 ± 7	7.6 ± 1	7.34 ± 1
288	21.4 ± 2	10.9 ± 2	9.5 ± 1	36.1 ± 8	20.7 ± 2	30.7 ± 6	36.1 ± 5	8.3 ± 1	7.0 ± 1
278	34.3 ± 1	7.9 ± 1	10.4 ± 1	54.2 ± 11	46.1 ± 6	54.7 ± 11	27.6 ± 3	5.8 ± 1	9.5 ± 1
243	52.7 ± 11	14.1 ± 2	19.6 ± 2	66.0 ± 28	50.3 ± 11	60.3 ± 21	96.5 ± 10	15.0 ± 1	23.2 ± 3

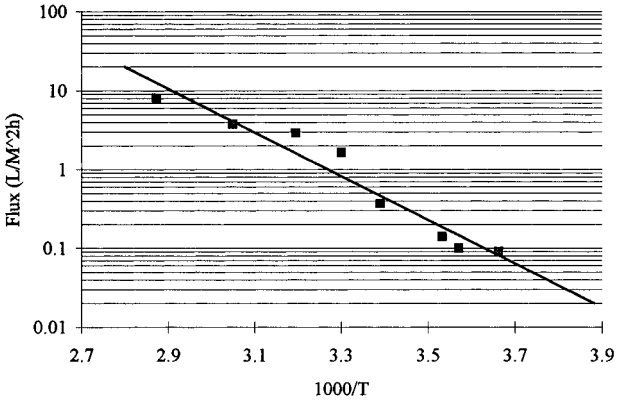

Figure 3. Arrhenius plot of 2-propanol permeation through a PPXP polymer. The line shown is a least-squares fit (R^2 = 0.941) that yields an activation energy of 53 kJ/mol.

Table 3. ^{13}C $T_{1\rho}$ Data for the Aromatic Region of the PPXP Polymer

	dry polymer (ms)		2-propanol swelled polymer (ms)	
temp (K)	quaternary (152 ppm)	methine aromatic (123 ppm)	quaternary (152 ppm)	methine aromatic (123 ppm)
358	25.8 ± 6	10.8 ± 1		
343	8.3 ± 0.2	4.5 ± 0.2		
323	5.1 ± 0.2	3.3 ± 0.5	16.1 ± 0.2	8.9 ± 0.6
308	12.7 ± 1	4.9 ± 0.4	4.9 ± 0.3	2.7 ± 0.03
298	43.1 ± 9	10.7 ± 2	6.9 ± 0.3	1.6 ± 0.1
288	26.3 ± 3	12.6 ± 2	10.8 ± 1	2.2 ± 0.1
278	32.0 ± 2	15.0 ± 4	25.6 ± 3	7.2 ± 1
263	27.8 ± 4	16.2 ± 1	85.8 ± 10	12.5 ± 2
243	68.4 ± 13	23.5 ± 5	60.8 ± 7	15.2 ± 2

chloride were purchased from Fisher and used as supplied. Deuterium oxide (99.8%D) was acquired from Cambridge Isotope Laboratories and used as received.

Glass transition temperatures were determined using a TA Instruments Model 2910 differential scanning calorimeter. ^{13}C and ^{1}H NMR spectra were collected using a Bruker AC-300P (proton frequency = 300 MHz) spectrometer equipped with a Bruker 7 mm double air bearing solid-state accessory and a VT-1000 temperature control unit (±0.1 K). ^{13}C spectra were taken at 75.5 MHz, a decoupling field of 58.9 kHz, and a CP contact time of 3000 μs. Variable temperature spectra were collected using standard Hartmann−Hahn conditions with at least 400 pulses and processed with 20 Hz exponential apodization. ^{1}H and ^{13}C $T_{1\rho}$ measurements were made using the method of Schaefer et al.[28,29]

Dry samples of PPOP were packed into a ZrO_2 rotor using standard techniques. Swelled samples were prepared by first soaking the polymer in solvent for at least 24 h. The sample was then packed into the rotor such that it was half full. Sample stability was maintained by the addition of glass wool to fill the remaining volume.

Samples of the PPXP were prepared from a casting solution of 8 wt % polymer and 3 wt % benzoyl peroxide (Aldrich Chemical Co.) in tetrahydrofuran. This solution was cast on a glass plate and allowed to dry followed by cross-linking in an oven at 473 K for 5 min. The polymers were removed from the glass by water floatation and dried under vacuum for at least 24 h. To prepare a sample for NMR analysis, the polymer film was powdered in a Tekmar laboratory mill equipped with a liquid N_2 jacket. Powdered polymers were dried under vacuum for at least 24 h before loading into the NMR sample rotor. The glass transition for this powder was measured at 26.9 °C. This T_g is consistent with samples of unpowdered dense film material.

The NOE difference experiments were performed using 70 mg of PPXP or PPOP placed in a 5 mm NMR tube followed by addition of 0.5 mL of deuterium oxide. Subsequently, 0.1 mL of methylene chloride was added by syringe and stirred on a vibration mixer for 10 min. NOE difference spectra were collected at 300, 310, and 320 K using an NOE difference pulse sequence[40] and 400 transients. Decoupling power was optimized to give maximum signal intensity without off-resonance excitation. To verify proper excitation, the on-resonance frequency was shifted 200 Hz, and the resulting difference spectrum showed no enhancement to the polymer resonances. Spectra were taken without sample spinning. Delays between transients were optimized at 8 s, 1−5 times the measured T_1 values. T_1 was measured using the inversion recovery method, and the value for the PPOP sample (broad singlet) was found to be 1.7 s. PPXP was observed to have a maximum T_1 of 2.6 s.

Results and Discussion

NMR Characterization Experiments. ^{13}C CP-MAS NMR spectra of dry PPOP were acquired over a variety of temperatures from 243 to 358 K. In the higher temperature acquisitions, four peaks were observed and assigned to the phenoxy pendant group (see Table 1). Line narrowing was observed as the temperature was increased as shown in Figure 1. In fact, the resonances attributable to the para and ortho carbons at 120 and 118 ppm, respectively, were not resolved until the temperature was above 308 K. The ipso carbon (148 ppm), for example, has a measured half-height line width of 200 Hz at 243 K and progressively narrowed to 100 Hz at 358 K. Similar behavior was noted for PPOP exposed to 2-propanol. Variable-temperature experiments were conducted from 243 to 323 K. Temperatures above 323 K were avoided due to evaporation concerns. Line narrowing was observed as the temperature was increased (Figure 1c). The line width for the ipso carbon was measured to be 200 Hz at 243 K and decreased to 100 Hz upon heating the sample to 323 K.

Variable-temperature acquisitions of THF-swelled PPOP were taken between 243 and 298 K, and the data are shown in Figure 1b. The data show enhanced resolution and narrow line width through all of the

(40) Derome, A. E. *Modern NMR Techniques for Chemistry Research*; Pergamon Press: Oxford, 1987; p 113.

Table 4. ^{13}C $T_{1\rho}$ Data for the *sec*-Butylphenol Substituent, Aliphatic Resonances

	dry polymer (ms)				2-propanol swelled polymer (ms)			
temp (K)	methine 37 ppm	CH_2 27 ppm	methyl 18 ppm	methyl 9 ppm	methine 37 ppm	CH_2 27 ppm	methyl 18 ppm	methyl 9 ppm
358	12.4 ± 4	16.5 ± 3	a	a				
343	2.0 ± 0.3	8.5 ± 1	15.1 ± 1	28.7 ± 3				
323	4.3 ± 2	6.7 ± 2	8.5 ± 0.4	11.0 ± 0.3	7.6 ± 0.4	11.9 ± 0.3	42.3 ± 5	*114 ± 53
308	4.6 ± 0.5	6.1 ± 1	10.8 ± 0.4	13.3 ± 0.2	7.9 ± 3	3.6 ± 0.4	9.2 ± 0.3	14.7 ± 1
298	8.6 ± 1	8.8 ± 1	17.3 ± 1	25.3 ± 2	2.1 ± 1	7.5 ± 1	8.5 ± 0.4	11.7 ± 1
288	15.3 ± 2	10.9 ± 1	31.4 ± 3	37.7 ± 3	1.9 ± 0.2	4.9 ± 0.3	9.4 ± 0.4	12.6 ± 1
278	17.5 ± 3	19.2 ± 3	23.9 ± 3	50.1 ± 7	6.1 ± 0.4	6.3 ± 0.3	12.8 ± 0.2	18.2 ± 1
263	20.5 ± 3	14.2 ± 2	21.3 ± 5	44.3 ± 5	13.9 ± 1	10.3 ± 1	21.8 ± 2	31.0 ± 1
243	19.0 ± 1	12.4 ± 1	39.4 ± 9	40.5 ± 2	13.7 ± 1	9.5 ± 1	16.9 ± 1	32.8 ± 2

[a] These data sets gave poor linear regressions with large errors, the slopes of these were very small, thus the $T_{1\rho}$'s are estimated to be in excess of 100 ms.

Table 5. ^{13}C $T_{1\rho}$ Data for the Methoxy Substituent, Methoxy Methyl Carbon

	methoxy methyl (51 ppm)	
temp (K)	dry polymer (ms)	2-propanol-swelled polymer (ms)
358	59.9 ± 9	
343	15.7 ± 0.3	
323	7.7 ± 0.2	26.5 ± 2
308	10.3 ± 0.2	10.7 ± 0.5
298	14.6 ± 2	8.7 ± 0.5
288	29.8 ± 2	8.7 ± 0.4
278	44.1 ± 3	16.0 ± 1
263	59.0 ± 11	31.0 ± 2
243	55.6 ± 5	38.7 ± 2

temperatures studied. In addition, there was less change in their line width due to temperature than was observed for the dry polymer or the 2-propanol-exposed sample. The half-height line width at 243 K was measured at 150 Hz, and this value decreased to 120 Hz at 298 K for the ipso-carbon resonances.

THF is considered a swelling solvent and a permeant for PPOP, while 2-propanol does not readily permeate. The fact that THF induces line narrowing through all of the observed temperatures suggests total solvation of the polymer pendant groups. Little effect is observed on the resonances when the polymer is exposed to 2-propanol suggesting minimal solvation. These data are consistent with the solution-diffusion theory as a contributor to the mechanism of polymer transport.

The terpolymer, PPXP, gave a solid-state ^{13}C NMR spectrum that was more complicated than the PPOP system. Spectral data assignments are shown in Table 1. The aliphatic region is dominated by five resonances that are attributable to the methyl group of *p*-methoxyphenol and the four carbons of the *sec*-butyl group. The aromatic region contains eight resonances, four quaternary carbons, and four protonated methine carbons.

Variable-temperature CPMAS experiments performed on PPXP showed the line width of the dry PPXP to be broadest at approximately 323 K for the aromatic, methylene, and methine carbons, while both above and below this temperature, the signals were more narrow (Figure 2). Methyl group rotation rates are influenced by temperature.[30] The most sterically unencumbered methyl groups were the γ-carbon of the *sec*-butyl group, 9 ppm, and the methoxy methyl carbon at 51 ppm in the ^{13}C spectrum. These resonances showed gradual narrowing with increasing temperature. For example, the half-height line width of the methoxy methyl carbon was 210 Hz at 243 K where it was only 50 Hz at 343 K. Steric influences were observed for the β-methyl carbon which was broad at 278 K and narrowed substantially

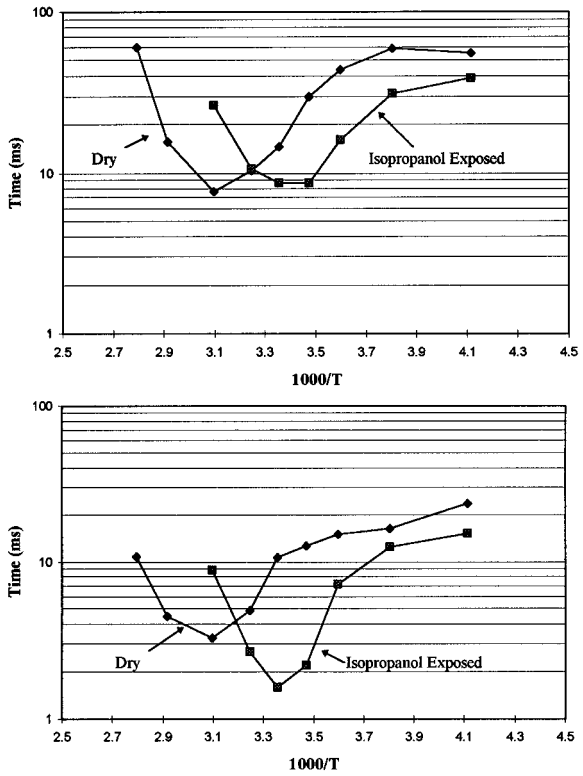

Figure 4. ^{13}C $T_{1\rho}$ versus temperature. The top figure shows data for the methoxy methyl carbon of the methoxy phenol substituent. The lower figure gives data for the broad methine aromatic signal, representing all three phenoxy substituents (*p*-methoxyphenol, *p*-*sec*-butylphenol, and *o*-allylphenol.)

up to 323 K. Measured half-height line width at 243 K was 310 Hz, and this value decreased to 55 Hz at 343 K. 2-Propanol-exposed PPXP was found to give variable-temperature spectra similar to the dry polymer; however, the temperature at which the line width was maximized for the aromatics, methine, and methylene was shifted to approximately 298 K (Figure 2b). Line broadening is attributed to incomplete motional averaging of the proton−carbon dipolar interactions.[37] The shift to lower temperature suggests that the reorientation rate for the pendant groups is increased with exposure to 2-propanol.

To further characterize the temperature dependence on polymer behavior, transport rates for 2-propanol through a PPXP polymer were studied. The data were collected using pervaporation with a polymer thickness of 30 μm and a transmembrane pressure of 500 mmHg. Flux rates were observed to increase an order of magnitude between 273 and 348 K (Figure 3). An Arrhenius plot of these data gives reasonable correlation

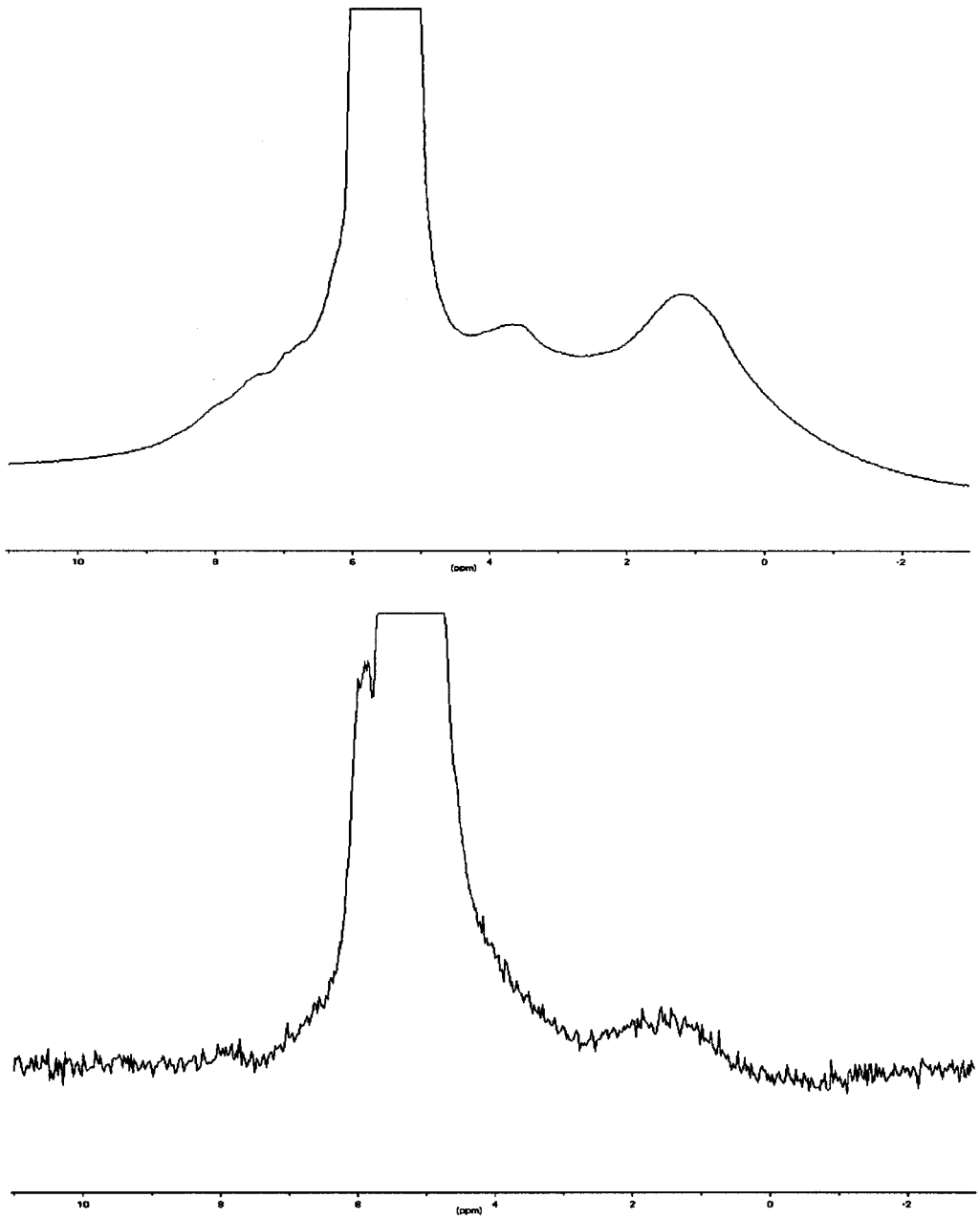

Figure 5. PPXP NOE experiment. Top spectrum is a reference ^{1}H spectrum of PPXP in $^{2}H_2O$ and CH_2Cl_2. The bottom spectrum is the NOE difference spectrum showing correlations to the methoxy resonance (3.8 ppm) and methyl groups (1.2 ppm).

and an activation energy of approximately 53 kJ/mol.

Solid-State NMR Relaxation Experiments. ^{13}C $T_{1\rho}$ parameters were acquired on several samples of PPOP. Over the temperature range observed, ^{13}C $T_{1\rho}$ values were found to vary little for the ortho and meta carbons of dry PPOP (see Table 2). ^{13}C $T_{1\rho}$ data acquired at 298 K were generally the shortest at approximately 8 ms and maxima that ranged from 20 to 30 ms were noted at the temperature extremes. The ipso-carbon ^{13}C $T_{1\rho}$ relaxation values were far more scattered and generally longer than those observed for the ortho and meta carbons, varying from 13 to 72 ms across the temperature profile. Protonated carbon relaxation times were generally shorter due to dipolar interaction with geminal protons. The 2-propanol-exposed PPOP experiments paralleled the dry PPOP samples suggesting little interaction between 2-propanol and the PPOP substrate. On the other hand, the THF swelling experiments showed more dramatic results. Increases in the ^{13}C $T_{1\rho}$ values were observed for the protonated carbons and correspond with solvation of the phenoxy substituents. The phenyl ipso carbons exhibited a smaller increase for the temperatures 243−298 K, suggesting that their relaxation is less influenced by solvation. Minima, as exhibited by both dry and 2-propanol-exposed samples, are proposed to be due to the molecular motion that is responsible for the lowered $T_{1\rho}$ relaxation times coinciding with the decoupling frequency of 58.9 kHz.[41] No minimum was observed for the THF experiment.

Similar experiments performed on dry PPXP gave ^{13}C $T_{1\rho}$ minima at 323 K (see Tables 2−4). For example, the ^{13}C $T_{1\rho}$ for the aromatic carbon at 123 ppm was 3.3 ms at 323 K (Table 3). This value increased to 10.8 ms

(41) Taylor, S. A.; White, J. L.; Elbaum, N. C.; Crosby, R. C.; Campbell, G. C.; Haw, J. F.; Hatfield, G. R. *Macromolecules* **1992**, *25*, 3369.

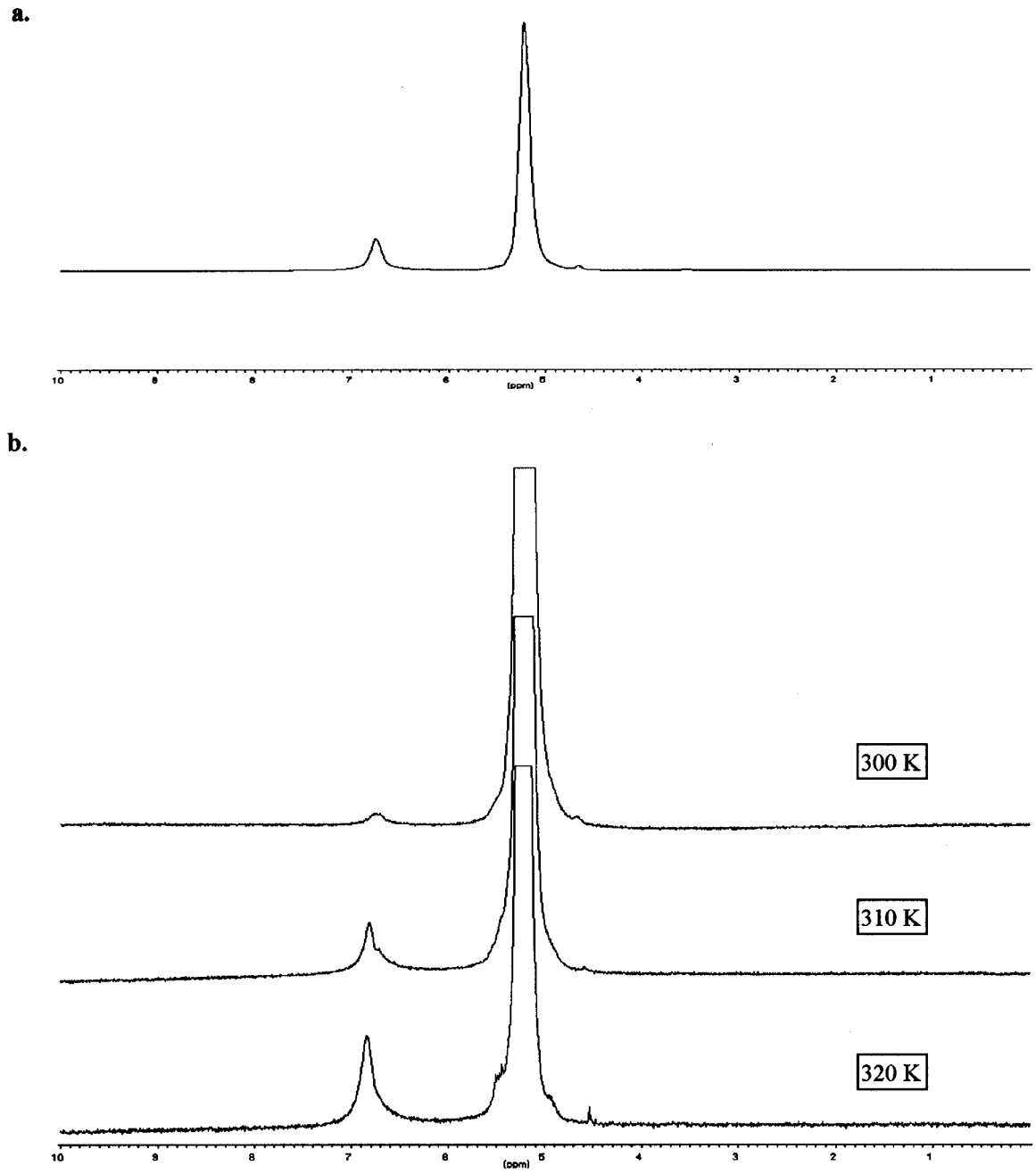

Figure 6. Variable-temperature NOE difference NMR spectroscopy performed on PPOP. (a) Reference ^{1}H spectrum at 300 K. (b) NOE difference spectrum at 300, 310, and 320 K. Assignments are PPOP (ortho, meta, and para protons overlapping) at 6.7 ppm, CH_2Cl_2 at 5.2 ppm, and H_2O at 4.6 ppm. Saturated resonance is the methylene chloride at 5.2 ppm.

at 358 K and 23.5 ms at 243 K. This trend was noted for all resonances, suggesting the influence of neighboring group motion upon relaxation. For the methoxy methyl carbon at 51 ppm, the minimum at 323 K was bracketed by increased relaxation times of 59.9 ms at 358 K and 59.0 ms at 283 K as shown in Table 5. This was observed to be a general trend as evidenced by the aromatic methine resonance (see Figure 4). Addition of isopropanol to PPXP induced a shift in the magnitudes of the ^{13}C $T_{1\rho}$, the minimum moved to lower temperature. For example, the minimum for the 123 ppm aromatic peak shifted to 298 from 323 K, as shown in Table 3. The general shape of the curve (Figure 6) remained consistent with the dry sample with increasing $T_{1\rho}$ relaxation times at both higher and lower temperatures. Likewise, the methoxy-methyl carbon also followed the same trend with minimum $T_{1\rho}$ value at about 293 K. $T_{1\rho}$ minima directly reflect relaxation due to molecular motion at the frequency of the spin-lock field (58.9 kHz).[41] Motions at that frequency occur at lower temperatures in the solvated system; thus it can be proposed that an isothermal comparison would yield higher motional frequencies for the solvent exposed system. This correlates well with polymer swelling as a process where the free volume increases due to solvent dissolution within the matrix.

Variable-temperature proton $T_{1\rho}$ experiments performed on PPOP gave fairly consistent data from 243 K to approximately 308 K (Table 5). At 308 K, ^{1}H $T_{1\rho}$ increases significantly. These data correspond to observed resonance line narrowing due to increased temperature. The signals for the ortho and para carbons observed near and below room temperature were not resolved; thus the data for these two resonances are

Table 6. ^{1}H $T_{1\rho}$ Data for PPOP Dry and Swelled in THF

	dry polymer (ms)			THF-swelled polymer (ms)		
temp (K)	ipso 148 ppm	meta 126 ppm	ortho 118 ppm	ipso 148 ppm	meta 126 ppm	ortho 118 ppm
323	28.4 ± 3	21.6 ± 1	30.4 ± 2	*a*	*a*	*a*
308	9.6 ± 1	6.0 ± 0.3	8.1 ± 1	*a*	*a*	*a*
298	4.9 ± 0.2	3.9 ± 0.1	4.5 ± 0.2	*a*	*a*	*a*
278	5.5 ± 1	3.7 ± 0.4	4.3 ± 1	*a*	*a*	*a*
263	4.2 ± 0.5	4.4 ± 1	3.6 ± 0.2	13.9 ± 3	16.8 ± 4	16.8 ± 5
243	5.0 ± 0.5	5.9 ± 0.4	3.9 ± 1	7.3 ± 0.5	10.4 ± 1	11.7 ± 2
223				7.5 ± 1	12.2 ± 1	12.3 ± 2
203				12.6 ± 0.3	15.0 ± 2	12.6 ± 1

[a] No clear decay of signal over the range of tau, slope is very small, it is estimated that the $T_{1\rho}$ is large.

presented as one peak in Table 6. The data from the dry PPOP were consistent for all observed carbons, reflecting efficient spin-diffusion. THF-swelled PPOP was studied from 203 to 323 K, and a similar flat region was measured between 203 and 263 K as shown in Table 6. It is proposed that the flat areas of the dry and THF swelled curves correspond with the similar shifts in ^{13}C $T_{1\rho}$ minima and can be attributed to solvation of the organic substituents on the polymer. Temperatures above 263 K gave data with poor linear behavior. The decay of the signal over the observation time (up to 12 μs) was nonexistent, so the ^{1}H $T_{1\rho}$ values are estimated to be large. This correlates to the sharp increases noted for the dry material at 308 K.

Liquid-State NMR Experiments. Difference NOE techniques were applied to samples of PPXP polymer with absorbed methylene chloride in deuterium oxide where the methylene chloride was irradiated. The difference spectrum clearly shows NOE enhancement to the aliphatic polymer resonances (see Figure 5). A specific dipole−dipole interaction between the solvent and aliphatics was reasonable due to their distant proximity from the crowded phosphorus−nitrogen polymer backbone.

PPXP showed broad signals in a difference NOE spectrum, the breadth of which made accurate determination of the amount of enhancement impossible, but it is estimated at less than 1%. A less than 1% NOE enhancement suggests that $K_{ex}/R_1 < 0.1$ where K_{ex} is the exchange rate of the methylene chloride on and off of the polymer at the locations that show enhancement and R_1 is the T_1 relaxation rate for the corresponding protons.[42] Therefore, the methylene chloride has a relatively fast exchange rate with PPXP. The observation of an NOE suggests the existence of a solvent sphere about the polymer pendant groups of at least 5 Å and that the magnitude of the NOE is a representation of the variable number of interacting solvent molecules and a distibution of intermolecular distances within the solvent sphere. These distributions, viewed through the NOE, change with respect to solvent, polymer, and temperature.

Figure 6 shows the one-dimensional reference ^{1}H NMR spectrum of PPOP polymer in a deuterated water/methylene chloride solvent mixture (70 mg of PPOP, 0.5 mL of H_2O-d_2, 0.2 mL of CH_2Cl_2). Two signals dominate the spectrum, PPOP is observed as a broad singlet representing overlapping signals from the ortho, meta, and para protons at 6.7 ppm and methylene chloride as a broad signal at 5.4 ppm. NOE enhancements of 3.9% at 300 K, 4.7% at 310 K, and 4.9% at 320 K were measured (Figure 6). In comparison to the PPXP experiments, a longer bound lifetime is observed for PPOP. The fact that enhancement was observed for the aromatic region infers that solvent penetrated between the aromatic rings connected to adjacent phosphorus atoms.

Interestingly, NMR signals are not observed for the polymer in water before addition of the methylene chloride. In addition, when methylene chloride is added to the water/PPOP mixture, it is readily absorbed by the polymer, and no separate methylene chloride layer is observed. Physical changes to the polymer were also observed. Before addition of the methylene chloride, PPOP appeared granular in the water, while afterward it agglomerated into a unified swollen mass within the sample tube.

Conclusion

Variable-temperature solid-state NMR data and $T_{1\rho}$ parameter determinations support the solution-diffusion theory of solvent transport through polyphosphazene materials. Increases in reorientation rates were observed for all carbons on pendant groups that are exposed to swelling solvent; conversely, nonswelling solvents were found to not exhibit rate increases. This suggests that solvent inclusion increases the free volume within the matrix. Heterogeneous NOE difference spectroscopy was used to observe a dipolar interaction between solvent and polymer substrate within a 5 Å solvent sphere, thus demonstrating solvent solubility within a polymer matrix. Application of this concept to membrane separations suggests permeating species must be intimately soluble in the polymer to be transported through it. The techniques outlined in this paper may allow for rapid determination of the nature of solvent swelling in a variety of other materials.

Acknowledgment. The work described in this paper was supported by the United States Department of Energy through Contract DE-AC07-94ID13223 and the INEL Laboratory Directed Research and Development Program..

CM960266Y

(42) Neuhaus, D.; Williamson, M. P. *The Nuclear Overhauser Effect in Structural and Conformational Analysis*; VCH Publishers, Inc.: New York, 1989; pp 141−181.